Neurotoxicity Research (2020) 38:287–298
https://doi.org/10.1007/s12640-020-00220-1

ORIGINAL ARTICLE

Thallium Toxicity in *Caenorhabditis elegans*: Involvement of the SKN-1 Pathway and Protection by *S*-Allylcysteine

María Ester Hurtado-Díaz[1,2] · Rubén Estrada-Valencia[1,2] · Edgar Rangel-López[1] · Marisol Maya-López[1] · Alinne Colonnello[1] · Sonia Galván-Arzate[3] · Sandra V. Verstraeten[4] · Cimen Karasu[5] · Isaac Túnez[6] · Michael Aschner[7] · Abel Santamaría[1]

Received: 17 January 2020 / Revised: 21 April 2020 / Accepted: 24 April 2020 / Published online: 28 May 2020

Abstract

Monovalent thallium (Tl^+) is a cation that can exert complex neurotoxic patterns in the brain by mechanisms that have yet to be completely characterized. To learn more about Tl^+ toxicity, it is necessary to investigate its major effects in vivo and its ability to trigger specific signaling pathways (such as the antioxidant SKN-1 pathway) in different biological models. *Caenorhabditis elegans* (*C. elegans*) is a nematode constituting a simple in vivo biological model with a well-characterized nervous system, and high genetic homology to mammalian systems. In this study, both wild-type (N2) and *skn-1* knockout (KO) mutant *C. elegans* strains subjected to acute and chronic exposures to Tl^+ [2.5–35 μM] were evaluated for physiological stress (survival, longevity, and worm size), motor alterations (body bends), and biochemical changes (glutathione *S*-transferase regulation in a gst-4 fluorescence strain). While survival was affected by Tl^+ in N2 and *skn-1* KO (worms lacking the orthologue of mammalian Nrf2) strains in a similar manner, the longevity was more prominently decreased in the *skn-1* KO strain compared with the wild-type strain. Moreover, chronic exposure led to a greater compromise in the longevity in both strains compared with acute exposure. Tl^+ also induced motor alterations in both *skn-1* KO and wild-type strains, as well as changes in worm size in wild-type worms. In addition, preconditioning nematodes with the well-known antioxidant *S*-allylcysteine (SAC) reversed the Tl^+-induced decrease in survival in the N2 strain. GST fluorescent expression was also decreased by the metal in the nematode, and recovered by SAC. Our results describe and validate, for the first time, features of the toxic pattern induced by Tl^+ in an in vivo biological model established with *C. elegans*, supporting an altered redox component in Tl^+ toxicity, as previously described in mammal models. We demonstrate that the presence of the orthologous SKN-1 pathway is required for worms in evoking an efficient antioxidant defense. Therefore, the nematode represents an optimal model to reproduce mammalian Tl^+ toxicity, where toxic mechanisms and novel therapeutic approaches of clinical value may be successfully pursued.

Keywords Thallium toxicity · Longevity · Survival · Oxidative damage · Nematodes · SKN-1

✉ Sonia Galván-Arzate
sonia_galvan@yahoo.com

✉ Abel Santamaría
absada@yahoo.com

[1] Laboratorio de Aminoácidos Excitadores, Instituto Nacional de Neurología y Neurocirugía, Insurgentes Sur 3877, 14269 Mexico City, Mexico

[2] Facultad de Ciencias, Universidad Nacional Autónoma de México, 04510 Mexico City, Mexico

[3] Departamento de Neuroquímica, Instituto Nacional de Neurología y Neurocirugía, 14269 Mexico City, Mexico

[4] Consejo Nacional de Investigaciones Científicas y Técnicas (CONICET), Instituto de Química y Fisicoquímica Biológicas (IQUIFIB), Facultad de Farmacia y Bioquímica, Universidad de Buenos Aires, C1113AAD Buenos Aires, Argentina

[5] Cellular Stress Response and Signal Transduction Research Laboratory, Faculty of Medicine, Department of Medical Pharmacology, Gazi University, Beşevler, 06500 Ankara, Turkey

[6] Departamento de Bioquímica y Biología Molecular, Facultad de Medicina y Enfermería, Instituto Maimónides de Investigación Biomédica de Córdoba (IMIBIC), Universidad de Córdoba, 14004 Córdoba, Spain

[7] Department of Molecular Pharmacology, Albert Einstein College of Medicine, Bronx, NY 11354, USA

Introduction

The toxicity of monovalent thallium cation (Tl^+) constitutes a major health issue worldwide, and this problem is worsened by its continued use for several industrial purposes (Galván-Arzate and Santamaría 1998; Blain and Kazantzis 2015; Osorio-Rico et al. 2017). Tl^+ acts on various organs, affecting cell metabolism at several levels, most prominently interfering with vital K^+- and Na^+-dependent processes (Favari and Mourelle 1985; Mulkey and Oehme 1993; Tao et al. 2008), promoting oxidative stress (Galván-Arzate et al. 2005; Korotkov 2009), and uncoupling mitochondrial oxidative phosphorylation (Melnick et al. 1976). In agreement, Tl^+ decreases endogenous antioxidant levels, increases ROS formation and lipid peroxidation, alters the mitochondrial membrane potential, causes mitochondrial depolarization and swelling with the consequent release of cytochrome c from mitochondria, and activates caspase 3, which ultimately leads to apoptosis (Eskandari et al. 2015; Pourahmad et al. 2010; Verstraeten 2006; Villaverde et al. 2004). In addition, Tl^+ causes PC12 cell mitochondrial depolarization and H_2O_2 formation, Bax oligomerization, and caspases 9 and 3 activation (Hanzel and Verstraeten 2006, 2009).

We have recently reported that Tl^+ recruits an excitotoxic component in its toxic pattern as evidenced by the ameliorative effects of selective in vivo blockade of *N*-methyl-D-aspartate receptors (NMDAr) on Tl^+-induced behavioral and biochemical toxic outcomes in rats (Osorio-Rico et al. 2015). In corroborative studies, we have recently demonstrated that the toxic effects elicited by Tl^+ in synaptosomal/mitochondrial fractions isolated from the rat brain were sensitive to the effects of endogenous NMDAr antagonist kynurenic acid, the cannabinoid receptor agonist WIN 55,212-2 and the antioxidant *S*-allyl-L-cysteine (Maya-López et al. 2018). Although these findings established the active participation of a conjugated excitotoxic/cannabinoid/oxidative component in the toxic pattern elicited by Tl^+, additional evidence in support of this concept and other toxic mechanisms is required, along with systematic characterization of various biological models, particularly under in vivo exposure conditions.

Caenorhabditis elegans (*C. elegans*) is a nematode representing a simple in vivo biological model since it exhibits practical characteristics such as small size, transparency, short life cycle, a wide variety of transgenic strains, and low cost of maintenance (Shashikumar et al. 2015). In addition, the neuronal network of the worm has been fully characterized (McVey 2010; Kim and Emmons 2017), thus providing evidence that it contains 302 neurons (Harrington et al. 2010). It is noteworthy that the SKN-1 antioxidant pathway expressed by *C. elegans* is homologous to the Nrf2/ARE antioxidant pathway in mammals (Blackwell et al. 2015; Kotlar et al. 2018; Cuadrado et al. 2019; Colonnello et al. 2019). The antioxidant defense system of the worm recruits SKN-1-mediated signaling to regulate a number of antioxidant enzymes and orchestrates integrated protection (An and Blackwell 2003; Martinez-Finley et al. 2013; Colonnello et al. 2019). In turn, SKN-1 deletions render the worm more sensitive to oxidative damage, thus favoring shorter lifespans (An and Blackwell 2003; Kotlar et al. 2018). Altogether, these and other characteristics establish *C. elegans* as an optimal alternative and complementary model to explore and characterize in vivo toxic mechanisms.

To our knowledge, no reports are available in literature exploring the toxic effects of Tl^+ in *C. elegans*, though the toxic mechanisms of several other metals (i.e., iron, copper, cadmium, and zinc) have already been characterized in this biological model (Queirós et al. 2019). Therefore, in this study we investigated the effects of Tl^+ on various endpoints of physiological stress, motor alterations, and biochemical changes in wild-type (N2) and *skn-1* KO mutant *C. elegans* strains subjected to acute and chronic exposures to Tl^+ as to validate the toxic features produced by this metal in vivo in the nematode.

Materials and Methods

Reagents and Strains

Thallium(I) acetate, HEPES, and *S*-allyl-L-cysteine (SAC) were obtained from Sigma-Aldrich Chemical Co. (St. Louis, MO, USA). Other reagents were obtained as reagent-grade from well-known commercial sources. Wild-type (N2; RRID:WB-STRAIN:RWK40N2) and mutant VC1772; *skn-1* KO ((ok2315)IV/nT1[qIs51](IV;V)) strains were both obtained from the Caenorhabditis Genetics Center (CGC, University of Minnesota, Minneapolis, MN). In addition, the CL2166 strain (dvIs19 [(pAF15)gst-4p::GFP::NLS]) was kindly provided by Eduardo Daniel Aguilar-Solis and Dr. Víctor Julián-Valdés (Instituto de Fisiología Celular, UNAM, Mexico). The experimental protocols were approved by the Ethics Committee for Animal Research of the Instituto Nacional de Neurología y Neurocirugía (Project No. 126/17). *Escherichia coli* strain (OP50-uracil auxotroph) was kindly provided by Dr. Rodolfo García Contreras from the Laboratorio de Bacteriología (Facultad de Medicina, UNAM, Mexico).

Nematode Culture

All *C. elegans* strains employed in this study were cultured at 21 °C on a Nematode Growth Medium (NGM) agar plate containing 0.6 g NaCl, 3.4 g agar (DIBICO, Mexico), 0.5 g Bacto Peptone (Becton Dickinson, Mexico), 0.5 M KH_2PO_4, 1 M $MgSO_4$, 1 M $CaCl_2$, 12 mM cholesterol, 1 mg/ml Nystatin (Perrigo Lab., Mexico), and 5 mg/ml Streptomycin

(PiSA, Mexico) plus an OP50 strain of *E. coli* as substrate. All strains were washed with sterile bi-distilled water from the NGM agar plate, followed by a lysis step with a 10 M NaOH/hypochlorite solution to obtain the eggs.

Thallium Content Analysis

The content of Tl^+ was measured in unwashed tissue fractions (pellets of ~ 300 μl) of nematodes that were treated with the metal (5 or 15 μM) for 1 h, as well as in supernatants (300 μl) collected immediately after the exposure to Tl^+, by centrifugation (5200*g* for 3 min). All tissue fractions were digested in 0.1 ml of HNO_3 Suprapur, as previously described (Ríos et al. 1989). Samples were analyzed by atomic absorption in a Graphite Furnace Atomic Absorption Spectrometer AA 600 Perkin-Elmer (Waltham, MA) with a coupled autosampler AS 800 and a Tl^+ hollow cathode lamp (276 nm of wavelength and slit of 0.7 nm). Argon flow (10 ml/min) served as a continuous purge gas during the analysis. Results were expressed as μg of Tl^+ per mg of wet tissue for tissue fractions, or as μg of Tl^+ per l for supernatants.

Treatments and Survival Test

Two thousand worms per assay of N2 (wild-type) and VC1772 (referred to as *skn-1* KO, according to Martinez-Finley et al. 2013) strains in L1 stage were exposed to graded doses of Tl^+ (2.5, 5, 10, 15, 20, 25, and 35 μM) for 1 h in Eppendorf tubes, further washed three times, and then cultured in NGM plates containing *E. coli* (OP50). Twenty-four hours after exposure, 3 high-density and 3 low-density worm cells were counted, and the average counting was multiplied by the total number of cells in order to obtain the number of worms in the plate. N2 worms with added SAC (1, 20, 50, 70, or 100 μM) pretreatment (added 30 min before the addition of 15 μM Tl^+) were also assayed. Six plates per treatment were analyzed for survival, and the procedure was repeated independently in triplicate, according to a previous report (Kotlar et al. 2018).

Longevity (Lifespan) Test in N2 and VC1772 Strains

Longevity test was performed according to previous reports (Amrit et al. 2014; Kotlar et al. 2018). Nematodes in L1 stage from both N2 and VC1772 strains were exposed to Tl^+ in 2 different schemes: (1) acute (one single exposure for 1 h at the beginning of the experiment), and (2) chronic (continuous exposure to the metal during the whole experiment, starting 24 h after synchronization (day zero)). For the chronic exposure experiment, worms were transferred into new plates containing the metal every 2 days, and the bacteria were exposed to UV light before worm seeding. All nematodes were grown on NGM-OP50 agar plates at 21 °C and observed daily for survival (until they died). Twenty worms from each group were followed throughout the experiments, and the assay was independently repeated in triplicate.

Locomotion Assessment in N2 and VC1772 Strains

Locomotion was assessed in the N2 and VC1772 strains 48 h after being exposed to acute doses of Tl^+. Locomotion was assessed as the number of body bends per worm, according to criteria established by Shashikumar et al. (2015), and recently reported by us (Colonnello et al. 2019). Nematodes picked up from the NGM-OP50 agar plate were transferred into a new NGM plate containing no bacteria; after 1-min adaptation, the number of bends in 1 min was quantified under a stereomicroscope. One body bend is defined as a change in direction of the cephalic region of a given worm, and this region can be distinguished by the presence of the pharyngeal bulb towards the right side. Each bend was counted only when the worm completed a whole undulatory movement. Eleven worms per group were tested, and tests were repeated independently 5 times in triplicate.

Body Size

The worm's body size was estimated as an index of morphological alterations after acute and chronic exposures to the metal. This parameter has been used by other authors in a previous report (Nagashima et al. 2016). Similar to the longevity assay, N2 and VC1772 strains in L1 stage were exposed to 5 or 15 μM Tl^+, either upon acute or chronic exposures. Images of representative worms from all groups were collected at different days of culture (3, 7, 10, 13, and 16), and served to calculate the worm size by analyzing the collected images using the ImageJ 1.50i software. Pixels were converted to length units (mm), and then expressed graphically.

Gst-4 Fluorescence in the CL2166 Strain

The *C. elegans* CL2166 strain carrying the reporter transgene Pgst-4::GFP was used for this experiment to fluorescently characterize the levels of Glutathione-*S*-Transferase (GST) transcription. After pretreatment with 20 or 50 μM SAC for 30 min, and/or exposure to 15 μM Tl^+ for 1 h, nematodes were transferred into Costar 96 Bottom Black Side plates to estimate the fluorescent intensity for GFP. Paralysis was induced to worms with ethanol (70%, − 20 °C), and GFP fluorescence was quantified at 485/20 nm in a Cytation3 Multiple Reader (BioTek, VA). Images of fluorescent worms were also taken with the Cytation3 Multiple Reader, and served to perform the densitometric analysis using the ImageJ 1.50i software.

Statistical Analysis

All experiments were conducted at least 3 times. Mean values ± standard error (SEM) were determined for all experiments. Statistical analyses were carried out using one- or multivariate analysis of variance, followed by post hoc Bonferroni's test, or Student *t* test, when appropriate.

Results

Tl^+ Exposure Increases its Levels in Nematode Tissue Pellets and Supernatants

As a first step, and in order to demonstrate that Tl^+ readily accumulates in the nematodes, its content was quantified in tissue pellets (Fig. 1a) and supernatants (Fig. 1b) of N2 worm cultures by atomic absorption spectrometry. As expected, Tl^+ was non-detectable in unexposed fractions, but was present both in tissue pellets (119 and 328 μg/mg of wet tissue for 5 and 15 μM, respectively; $P \leq 0.01$, 15 μM vs. 5 μM) and supernatants (949 and 2335 μg/l for 5 and 15 μM, respectively; $P \leq 0.01$, 15 μM vs. 5 μM), and its content was increased in a dose-dependent manner in both fractions. The presence of Tl^+ in the tissue pellets after a 1-h exposure demonstrated the take up of the metal by worms from the medium.

Survival of N2 and VC1772 Strains Was Reduced by Increased Dosing with Tl^+

Figure 2 depicts the effects of growing concentrations of Tl^+ [2.5–35 μM] on the percent of survival of N2 and VC1772 *C. elegans* strains. In both cases, all concentrations of Tl^+ assessed decreased significantly worm survival ($P \leq 0.01$–$P \leq 0.0001$), compared with their respective controls. In the case of the N2 strain, Tl^+ induced a concentration-response effect, with the maximum toxic effect observed at concentrations ranging from 15 to 35 μM (41–44% below the control; $P \leq 0.0001$). In contrast, in the VC1772 strain, Tl^+ induced a U-shape effect, with a maximum toxic effect observed at the 10 μM concentration (40% below the control; $P \leq 0.0001$). When comparing N2 with VC1772, statistical differences were found at the 10, 15, and 35 μM concentrations of Tl^+ ($P \leq 0.05$). No differences were found in the survival rate between the control (untreated) groups of N2 and VC1772.

Acute and Chronic Exposure to Tl^+ Decreased Longevity in a Strain-Specific Manner

Figure 3 depicts longevity curves in N2 and VC1772 *C. elegans* strains exposed to 5 or 15 μM Tl^+ in acute (**a**) and chronic (**b**) experimental protocols. In both cases, VC1772 controls showed marked reduction in their lifespan (18 days) respect to N2 controls (25 days); and these differences were evident commencing on day 10 and throughout the rest of the experiment ($P \leq 0.0001$, VC1772 vs. N2).

As shown in Fig. 3a, after acute exposure to the metal, longevity in N2 worms was slightly decreased by 5 μM Tl^+ commencing on day 15, and completely compromised by 15 μM by day 10. Statistical differences were observed only for 15 μM Tl^+ compared with control worms between days 12 and 16 ($P \leq 0.01$). Maximal longevities for 5 and 15 μM N2 Tl^+-treated worms were 22 and 21 days, respectively, shorter than the 24-day lifespan of the controls. Changes in VC1772 lifespan caused by Tl^+ were less intense compared with its own control (significant changes found only for 15 μM Tl^+ vs. the control at days 8 and 9 ($P \leq 0.05$)), with maximal longevities of 18 and 17 days for 5 and 15 μM Tl^+, respectively, and 18 days for its own control.

As shown in Fig. 3b, after chronic exposure to Tl^+ 5 and 15 μM, the lifespan of N2 worms was significantly decreased commencing on day 10 compared with their own control. Statistical differences were observed for 5 μM Tl^+ compared with control worms at days 12 and 13 ($P \leq 0.05$), and for 15 μM Tl^+ compared with control worms between days 11 and 13 ($P \leq 0.01$). Maximal longevities for the two tested doses of Tl^+ in the N2 strain were 19 and 17 days, respectively, shorter than the 24 days found in the control. Both 5 and 15 μM Tl^+ reduced the longevity in the VC1772 strain at different time points, 15 μM being more lethal than 5 μM (significant changes found for 5 μM Tl^+ vs. the control at days 9 and 10 ($P \leq 0.05$), and for 15 μM Tl^+ vs. the control at day 12 ($P \leq 0.01$)). Maximal longevities in the VC1772 strain were 14, 17, and 18 days for the 5 μM and 15 μM Tl^+, and the control, respectively.

In general, VC1772 was statistically different from N2 in both acute and chronic exposures (ranging $P \leq 0.05$–$P \leq 0.0001$ at different time points). In addition, comparing the longevity in Fig. 3a with Fig. 3b (acute vs. chronic), it is evident that chronic exposure to Tl^+ affected the outcome of N2 and VC1772 strains in a more intense manner than acute exposure, as evidenced by the progression and maximal points of longevity reached in both experimental approaches (ranging $P \leq 0.05$–$P \leq 0.0001$ at different time points).

Tl^+ Exposure Induced Motor Alterations in the N2 and VC1772 Strains

Figure 4 depicts the effect of increased acute dosing with Tl^+ (2.5–35 μM) on the number of body bends (motor/behavioral activity) as an index of behavioral activity in nematodes from both N2 and VC1772 strains. The number of body bends in

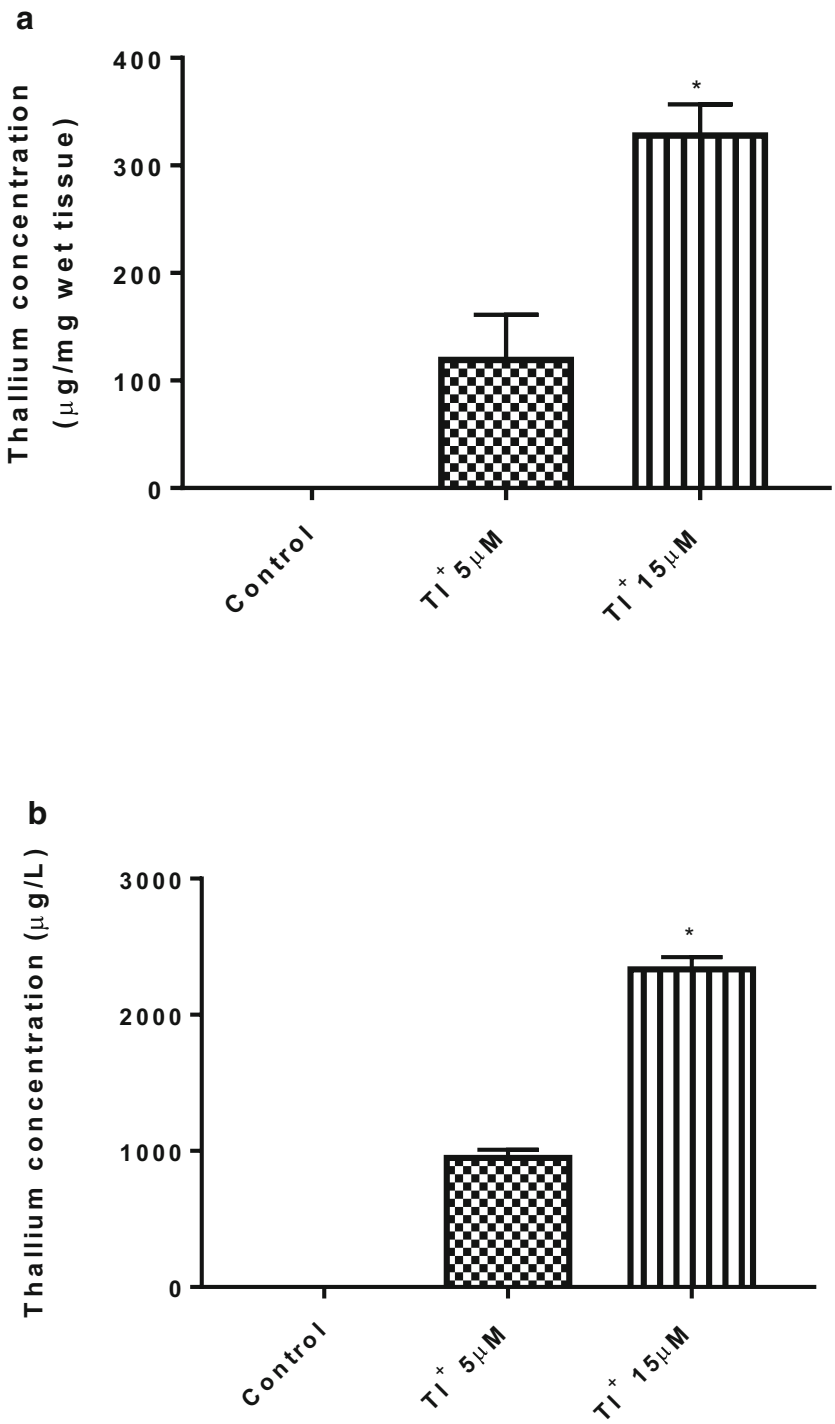

Fig. 1 Thallium content in liquid fractions obtained from tissue pellets (**a**) and supernatants (**b**) of culture media containing *C. elegans* N2 worms exposed for 1 h to thallium(I) acetate (5 or 15 μM). Results are shown as the mean ± SEM of $n = 8$ experiments per group. *$P \leq 0.01$, 15 μM significantly different from 5 μM; Student's *t* test

the untreated VC1772 group was 22% lower than those of the untreated (control) N2 group ($P \leq 0.01$). For both N2 and VC1772 strains, Tl^+ induced a U-shape effect on motor activity, with maximal alterations observed at 15 μM (53% and 41% lower than their controls for N2 and VC1772, respectively; $P \leq 0.0001$). In addition, at all doses tested, Tl^+ induced a more intense reduction in motor activity in the VC1772 strain compared with the N2 strain ($P \leq 0.05$–$P \leq 0.0001$).

Tl^+ Induced Changes in the Worm Size in the N2 Strain

As shown in Table 1, the standard size of the N2 strain (control; ~ 1.2-mm length) was not affected by the acute (A) exposure to Tl^+ for 1 h and measured 3 days later. In contrast, chronic (C) exposure to the metal for 3 days caused marked decrease in body size, with values 16% and 17% below the control ($P \leq 0.01$) for 5 and 15 μM Tl^+, significantly.

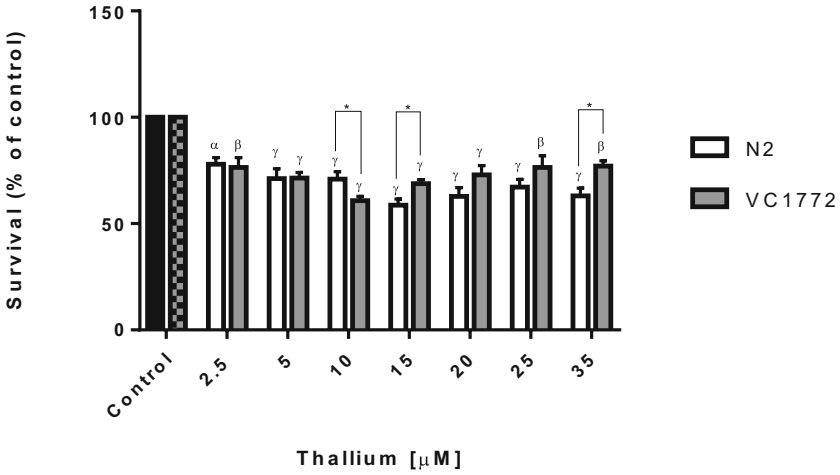

Fig. 2 Effect of increasing doses of thallium(I) acetate on survival of *C. elegans* N2 (black and white bars) and VC1772 (squared and gray bars) strains. Values represent means ± S.E.M. of $n = 6$ experiments per group. $^{\alpha}P \leq 0.01$, $^{\beta}P \leq 0.001$, and $^{\gamma}P \leq 0.0001$, significantly different from its own control. $^{*}P \leq 0.05$, significantly different from the value measured in N2 strain; multivariate ANOVA followed by Bonferroni's test

As shown in Table 2, exposure of the N2 strain to 15 μM Tl^+ (but not 5 μM) for 1 h (A) decreased the worm size in 21% compared with the standard size measured at day 16 ($P \leq 0.01$, different from the control group). No data are displayed for the continuous (C) exposure of worms to Tl^+ for 16 days since, as at such time, no live worms were found in the media. The worm size was also measured in nematodes from the VC1772 strain exposed to Tl^+, but no changes were found (data not shown).

The Tl^+-Induced Reduction in the Survival Rate in the N2 Strain Was Prevented by the Antioxidant SAC

Increased dosing (1, 20, 50, 70, and 100 μM) with the antioxidant SAC attenuated the Tl^+-induced decrease in survival rate in N2 worms as shown in Fig. 5. Tl^+ (15 μM) decreased survival by 52% compared with the control group ($P \leq 0.0001$). All tested SAC doses led to a significant attenuation in the Tl^+-induced survival rate loss ($P \leq 0.0001$;

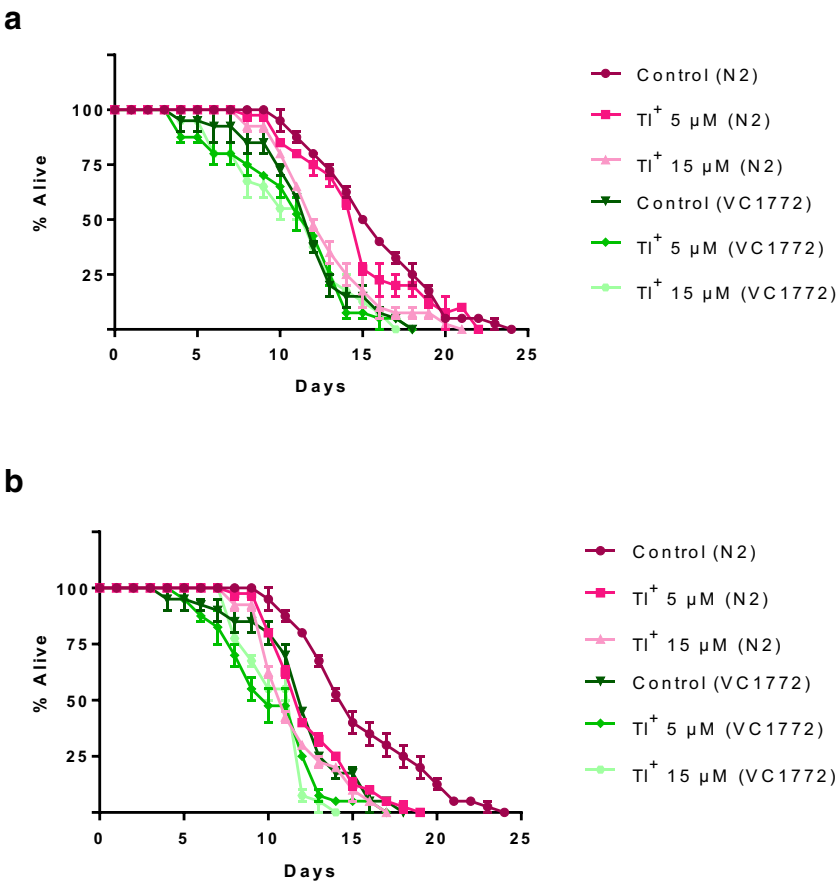

Fig. 3 Acute (**a**) and chronic (**b**) effects of thallium(I) acetate (5 and 15 μM) on longevity of *C. elegans* N2 and VC1772 strains. Individual points represent the mean value ± S.E.M. of $n = 20$ experiments per group per time point. Statistical significances (calculated by multivariate ANOVA) are indicated in the text

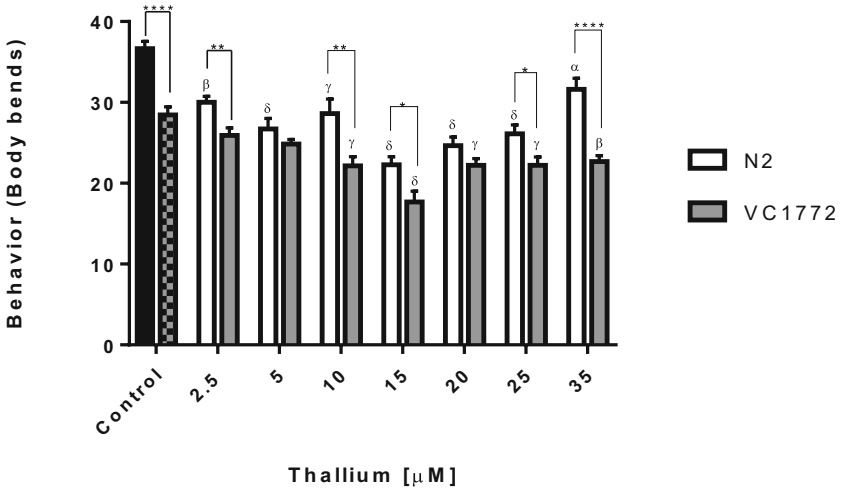

Fig. 4 Effect of increased doses of thallium(I) acetate on locomotion rate (body bends/min) and worm size in *C. elegans* N2 (black and white bars) and VC1772 (squared and gray bars) strains. Values represent means ± S.E.M. of $n = 10–13$ experiments per group. $^{\alpha}P \leq 0.05$, $^{\beta}P \leq 0.01$, $^{\gamma}P \leq 0.001$, and $^{\delta}P \leq 0.0001$ vs. its own control. $^{*}P \leq 0.05$, $^{**}P \leq 0.01$, and $^{****}P \leq 0.0001$, VC1772 different from N2; multivariate ANOVA followed by Bonferroni's test

different from the Tl^+ group), though there was no dose dependence associated with the SAC pretreatment (29–33% of protection compared with the Tl^+ group). SAC alone did not modify the survival of the control group (data not shown).

SAC Prevented the Decrease of GST Expression Induced by Tl^+ in the *C. elegans* CL2166 Strain

Worms from the CL2166 strain carrying the reporter transgene Pgst-4::GFP as a reporter for GST transcription were exposed to 15 μM Tl^+ and/or SAC (20 or 50 μM), and the expression and intensity of fluorescence were recorded (Fig. 6). As shown in the top part of the figure, Tl^+ reduced the total GST expression in ~ 70% compared with the control group ($P \leq 0.001$). In contrast, pre-incubation of worms with 20 μM SAC completely prevented the Tl^+-induced loss of GFP (182% respect to Tl^+ group; $P \leq 0.0001$), whereas 50 μM SAC + Tl^+ increased in 57% the expression of GST compared with the control group (57% above; $P \leq 0.0001$). This finding suggests that SAC upregulates the expression of this enzyme as part of the integral antioxidant response evoked by the antioxidant compound. These quantitative results were obtained from representative worms observed in culture dishes, and they are shown in the bottom panels of the same figure. SAC alone did not affect basal fluorescence (data not shown).

Discussion

Results obtained in this study corroborate previous reports showing that, at micromolar concentrations, Tl^+ triggers apoptotic pathways in PC12 cells (Hanzel and Verstraeten 2009) and induces mitochondrial dysfunction in rat brain synaptosomes (Maya-López et al. 2018). Tl^+-induced oxidative damage and disruption of antioxidant defense systems has been observed under different experimental conditions (Galván-Arzate et al. 2005; Hanzel and Verstraeten 2006; Osorio-Rico et al. 2015), and might be related to different toxic mechanisms, including its ability to interfere with the activity of Na^+/K^+-ATPase (Osorio-Rico et al. 2015; Maya-López et al. 2018), its capacity to induce hydrogen peroxide generation through impaired mitochondrial function (Hanzel and Verstraeten 2006), and its role in ROS formation, as well as the decrease of reduced glutathione (GSH) levels and glutathione peroxidase activity (Hanzel and Verstraeten 2006, 2009; Verstraeten 2006; Osorio-Rico et al. 2015; Pourahmad et al. 2010; Pino et al. 2017). In addition, Tl^+-induced disrupted ionic transport via alteration of membrane proteins is known to interfere with Na^+ and K^+ gradients (Favari and Mourelle 1985; Tao et al. 2008; Blain and Kazantzis 2015), which, in turn, might account for the loss of cell homeostasis that leads to oxidative damage. Whether analogous mechanisms characterize these changes in the nematode has yet to be investigated. With regard to several of the endpoints addressed herein, such as survival and behavior, which were

Table 1 Worm size (mm) in N2 strain after acute (A) and chronic (C) exposure to Tl^+ (5 and 15 μM) at day 3 of culture

Control (A)	Tl^+ 5 μM (A)	Tl^+ 15 μM (A)	Control (C)	Tl^+ 5 μM (C)	Tl^+ 15 μM (C)
1.20 ± 0.04	1.20 ± 0.05	1.14 ± 0.06	1.20 ± 0.03	1.03 ± 0.02^{A}	1.02 ± 0.04^{A}

Values represent means ± SEM of $n = 5–10$ experiments per group

$^{A}P \leq 0.01$, different from its own control; one-way ANOVA followed by Bonferroni's test

Table 2 Worm size (mm) in N2 strain after acute (A) and chronic (C) exposure to Tl^+ (5 and 15 μM) at day 16 of culture

Control (A)	Tl^+ 5 μM (A)	Tl^+ 15 μM (A)	Control (C)	Tl^+ 5 μM (C)	Tl^+ 15 μM (C)
1.42 ± 0.05	1.37 ± 0.05	1.13 ± 0.06*	1.22 ± 0.06[A]	-	-

Values represent means ± SEM of $n = 5–10$ experiments per group

[A] $P \leq 0.01$, different from its own control

*$P \leq 0.05$, 15 μM different from 5 μM; one-way ANOVA followed by Bonferroni's test

clearly affected in response to metal exposure, we noted a U-shaped response, suggesting hormetic response to counteract the toxic actions of Tl^+—possibly targeting oxidative stress and inflammatory pathways by recruiting heat-shock proteins, antioxidant enzymes, growth factors, and metalloproteins, as typically described for this phenomenon (Calabrese and Baldwin 2001; Mattson 2008; López-Diazguerrero et al. 2013; Elmazoglu et al. 2020; Hauser-Davis et al. 2020). Nonetheless, these endpoints did not exhibit full recovery (return to basal levels), validating the toxic potency of Tl^+.

The use of simple biological models for toxicological research constitutes a valuable experimental alternative for the understanding of toxic mechanisms. Surprisingly, no studies on Tl^+ toxicity have been previously reported in *C. elegans*, though the effects of other metals (manganese, methylmercury, iron, cadmium, lead, etc.) have been studied (Lu et al. 2018; Soares et al. 2018; Schetinger et al. 2019; Tang et al. 2019). Despite the fact that (1) thallium can be present as Tl^+ and Tl^{3+} species in biological systems challenged with the metal; (2) these two species exert different degrees of toxicity probably due to their capacity to alter the content of thiols in proteins in a differential manner, as well as by other mechanisms such as selective triggering of intrinsic and extrinsic apoptotic pathways (Hanzel and Verstraeten 2009; Pourahmad et al. 2010); and (3) the possibility that Tl^+ may be oxidized to Tl^{3+}—although this has not been described in the higher species, but only in certain species of plankton (Twining et al. 2003) due to the high oxidative potential required (+ 1.25 V)—, our interest in this study aimed to test the metal toxicity derived from the initial addition of Tl^+ to nematodes since this cation itself is relevant as an environmental pollutant and has been shown to be responsible for toxicity upon different experimental scenarios (Hanzel and Verstraeten 2009; Pourahmad et al. 2010; Maya-López et al. 2018). Moreover, though Tl^+ toxicity has already been tested in other species of invertebrates (including the planktonic crustacean *Daphnia pulex* (Tatsi et al. 2015), the water flea *Ceriodaphnia dubia* (Rickwood et al. 2015), the fly *Chironomus riparius* (Belowitz et al. 2014), the algae *Chlorella sp.*, and the cyanobacteria *Synechococcus*

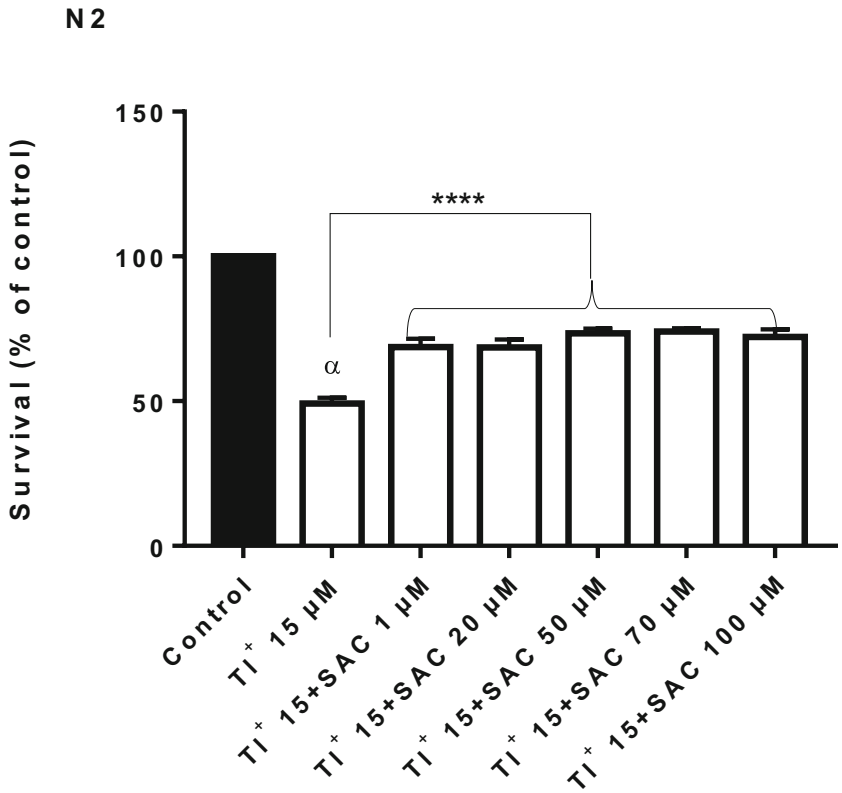

Fig. 5 Effect of increased doses (1–100 μM) of *S*-allylcysteine (SAC) on thallium(I) acetate (15 μM)-induced changes in survival in *C. elegans* N2 (WT) strains. Values represent means ± SEM of $n = 6$ experiments per group. $^{\alpha}P \leq 0.0001$, different from the control; ****$P \leq 0.0001$, different from Tl^+; multivariate ANOVA followed by Bonferroni's test

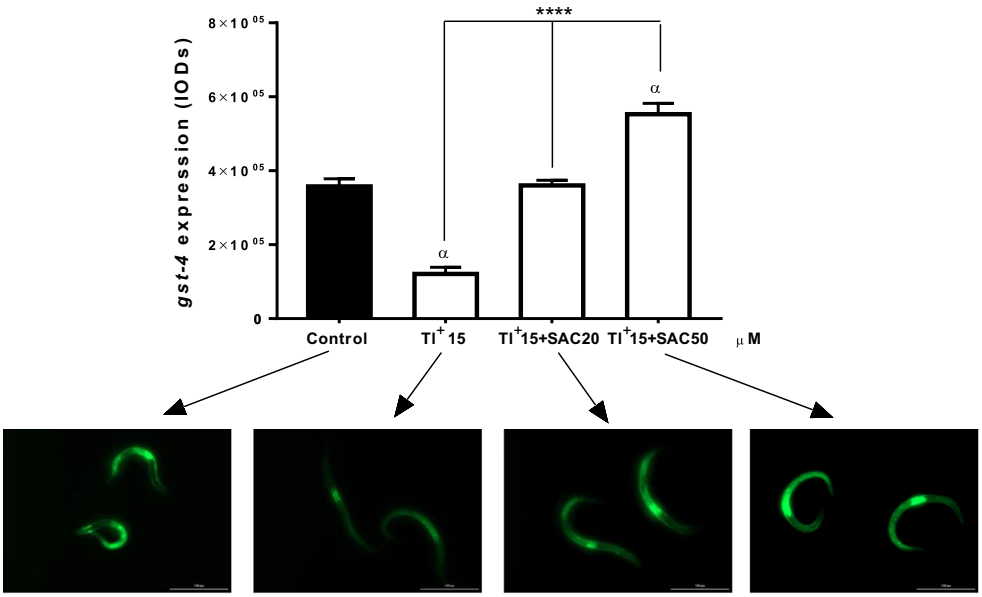

Fig. 6 Effects of 20 or 50 μM *S*-allylcysteine (SAC) on gst-4 fluorescence in *C. elegans* CL2166 strain. Values represent means ± SEM of $n = 6$ experiments per group. $^{\alpha}P \leq 0.001$ vs. the control; $^{****}P \leq 0.0001$ vs. Tl^{+}; multivariate ANOVA followed by Bonferroni's test. Bottom panel shows representative images of gst-4 expression (green fluorescent signal) in worms. Micrographs correspond to × 20 magnifications

leopoliensis (Hassler et al. 2007; Turner and Furniss 2012)), the worm model has obvious advantages over the formers as it allowed the evaluation of physiological alterations, not only at the biochemical and behavioral levels but also at the molecular one since the contribution of the selected mutation skn-1 was also investigated. The *skn-1* mutation was associated with an increase in the toxic effects evoked by Tl^{+} in nematodes. In turn, the SKN-1 pathway regulates the expression of GST-4 in *C. elegans* (Detienne et al. 2016), and since Tl^{+} decreased GST-4 expression in the CL2166 strain, it is plausible that this cation could repress in vivo the expression of *skn-1* gene, thus depressing the glutathione-dependent antioxidant defense system.

The contribution of the compromised SKN-1 pathway to other toxic models (including metals such as methylmercury and iron, neurotoxins such as quinolinic acid and 6-hydroxydopamine, and pathological conditions such as obesity) has already been tested and described (Martinez-Finley et al. 2013; Ushiama et al. 2016; Colonnello et al. 2019). For Tl^{+}, we hypothesize that oxidation of thiols induced by a previously generated oxidative stress produced by this cation might activate the SKN-1 pathway; in this context, the absence of this pathway in the *skn-1* KO strain might potentiate Tl^{+} toxicity given the lack of signaling mediated by oxidized thiols and the ensuing activation of cytoprotective/antioxidant genes, as it has been suggested for methylmercury (Aschner and Aschner 2007). Our results also demonstrate that Tl^{+}-induced toxicity is tightly related with the SKN-1 pathway, as has been demonstrated for other metals such as methylmercury (Chen et al. 2019). In further support to this concept, the use of SAC as a pharmacological tool to reduce oxidative damage corroborates the role that ROS exert on the Tl^{+}-induced nematode cytotoxicity and death in nematodes, as it has been previously demonstrated in *C. elegans* (Ogawa et al. 2016) and in mammals (García et al. 2014; Shi et al. 2015; Maya-López et al. 2018). In addition, SAC is known to reduce the toxic effects of toxic metals such as cadmium (Boonpeng et al. 2014), copper, and other heavy metals (Pedraza-Chaverrí et al. 2004; Flora 2009). SAC has been shown to scavenge free radicals and stimulate the transactivation of the Nrf2 transcription factor in mammals, thus generating an integral antioxidant and cytoprotective response (Colín-González et al. 2015). Organosulfur compounds, such as SAC, have been shown to exert several protective effects. Besides of the obvious capacity that SAC possesses to scavenge free radicals and probably chelating metals through its thioallyl structure, other structural groups within, including the alanyl group (−CH2CH−NH2−COOH), have been shown to confer additional protective properties under toxic conditions, such as oxygen glucose deprivation and global cerebral ischemia (Kim et al. 2006). Furthermore, significant correlations have been found between the in vivo neuroprotective activity of SAC and the reactive oxygen species scavenging activities.

As a result of the SAC-induced stimulation of integral antioxidant responses, the survival, longevity, and motor activity were significantly improved in Tl^{+}-exposed worms; however, whether SAC can induce the SKN-1 pathway activation in nematodes remains to be investigated. Recently, it was proposed that one of the toxic mechanisms of thallium may be associated with decreased antioxidant defense capacity in living organisms, which can be associated with the formation of Tl^{3+} ions in interacting of Tl^{+} with ROS molecules produced near the centers of the respiratory chain of mitochondria (Korotkov et al. 2015; Korotkov et al. 2016). Moreover, Tl^{3+}, but not Tl^{+}, is capable to oxidize molecular thiol groups, including GSH (Bunni and

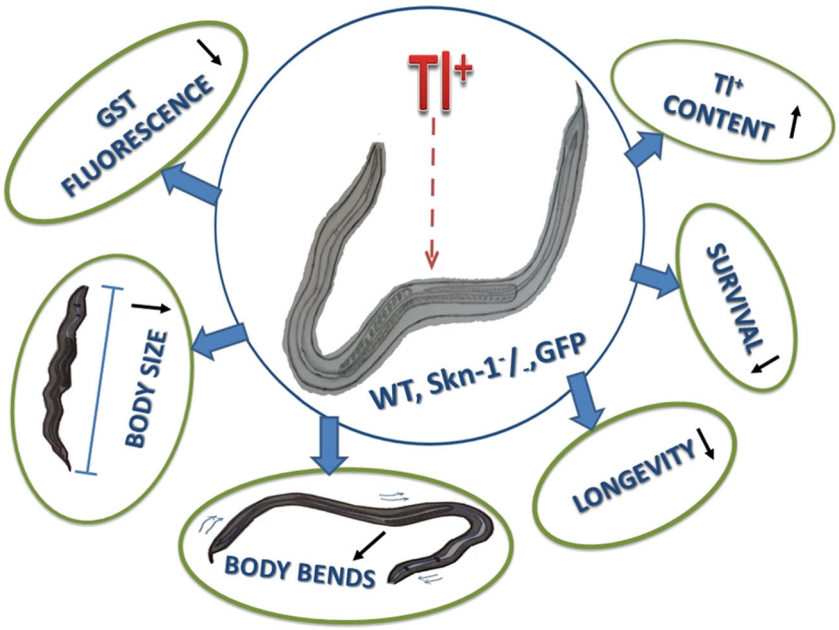

Fig. 7 Schematic representation of the toxic effects exerted by thallium(I) acetate in *C. elegans* nematodes

Douglas 1984; Khan et al. 2018), although the possibility that Tl^+ decreases GSH content by abstracting an electron from the sulfhydryl moiety with the generation of a thiyl radical has been proposed (Pourahmad et al. 2010). Thus, another reason for the decrease in the toxic effects of thallium in these nematodes may be due to the scavenging of ROS molecules by *S*-allylcysteine after thallium toxicity. Contrasting the findings of this study with observations previously described on Tl^+-induced cellular and redox alterations in the mammalian CNS (Villaverde et al. 2004; Galván-Arzate et al. 2005; Maya-López et al. 2018; Lin et al. 2020), our results demonstrate that, analogous to mammals, the toxic pattern evoked by Tl^+ in *C. elegans* is mediated by a redox-altered component linked to antioxidant signaling regulation. For further experimental approaches on toxicological studies with thallium in the *C. elegans* nematode model, it should be considered that bacterial content in the culture medium, which is used to feed the worms, could affect the toxicity of the metal, as it has been demonstrated for methylmercury in the same animal model (Ke and Aschner 2019); therefore, methodological approaches should be improved from this point on.

To summarize, main findings obtained in the present study are represented in Fig. 7 aimed to indicate that the uptake of Tl^+ by the nematodes leads to Tl^+ deposition in the tissues that impairs a key antioxidant defense system and that ultimately affects their body size, motility, and lifespan.

Concluding Remarks

Herein, for the first time, we describe Tl^+-induced toxic effects on major physiological, behavioral, and biochemical endpoints in *C. elegans*. These effects were associated to the disruption of redox balance, as demonstrated by the augmented toxicity linked to *skn-1* KO mutation, as well as the ameliorative response of nematodes towards the antioxidant SAC. Combined, these results establish the nematode as an accurate and suitable biological model for investigating noxious mechanisms and associated signaling pathways linked to in vivo Tl^+ toxicity. These findings open new venues for research on Tl^+-induced toxicity and contribute to the understanding of heavy metal poisoning at the experimental and clinical levels, leading to the development of new pharmacological modalities for the treatment of metal-induced toxicity.

Funding Information MA was supported in part by grants from the National Institute of Environmental Health Sciences, R01ES03771, R01ES10563, and R01ES020852. Financial support was also given to SVV from the Agencia Nacional de Promoción Científica y Tecnológica (ANPCyT; PICT2017-1861).

Compliance with Ethical Standards

Conflict of Interest The authors declare that they have no competing interests.

References

Amrit FR, Ratnappan R, Keith SA, Ghazi A (2014) The C. elegans lifespan assay toolkit. Methods 68:465–475

An JH, Blackwell TK (2003) SKN-1 links C. elegans mesendodermal specification to a conserved oxidative stress response. Genes Dev 17:1882–1893

Aschner JL, Aschner M (2007) Methylmercury neurotoxicity: exploring potential novel targets. Open Toxicol J 1:1–9

Belowitz R, Leonard EM, O'Donnell MJ (2014) Effects of exposure to high concentrations of waterborne Tl on K and Tl concentrations in

Chironomus riparius larvae. Comp Biochem Physiol C Toxicol Pharmacol 166:59–64

Blackwell TK, Steinbaugh MJ, Hourihan JM, Ewald CY, Isik M (2015) SKN-1/Nrf, stress responses, and aging in *Caenorhabditis elegans*. Free Radic Biol Med 88(Pt B):290–301

Blain R, Kazantzis G (2015) Thallium. In: Nordberg GF, Fowler BA, Nordberg M (eds) Handbook on the Toxicology of Metals. Volume II: Specific Metals. Academic Press, Elsevier, Amsterdam 1229–1240 pp

Boonpeng S, Siripongvutikorn S, Sae-Wong C, Sutthirak P (2014) The antioxidant and anti-cadmium toxicity properties of garlic extracts. Food Sci Nutr 2:792–801

Bunni MA, Douglas KT (1984) Arylthallium(III) reagents for protein modification. Inhibition of lactate dehydrogenase from various sources by o-carboxyphenylthallium(III) bistrifluoroacetate. Biochem J 217:383–390

Calabrese EJ, Baldwin LA (2001) U-shaped dose-responses in biology, toxicology, and public health. Annu Rev Public Health 22:15–33

Chen M, Wang F, Cao JJ, Han X, Lu WW, Ji X, Chen WH, Lu WQ, Liu AL (2019) (−)-Epigallocatechin-3-gallate attenuates the toxicity of methylmercury in Caenorhabditis elegans by activating SKN-1. Chem Biol Interact 307:125–135

Colín-González AL, Ali SF, Túnez I, Santamaría A (2015) On the antioxidant, neuroprotective and anti-inflammatory properties of S-allyl cysteine: an update. Neurochem Int 89:83–91

Colonnello A, Aguilera-Portillo G, Rubio-López LC, Robles-Bañuelos B, Rangel-López E, Cortez-Núñez S, Evaristo-Priego Y, Silva-Palacios A, Galván-Arzate S, García-Contreras R, Túnez I, Chen P, Aschner M, Santamaría A (2019) Comparing the neuroprotective effects of caffeic acid in rat cortical slices and *Caenorhabditis elegans*: involvement of Nrf2 and SKN-1 signaling pathways. Neurotox Res In Press 37:326–337. https://doi.org/10.1007/s12640-019-00133-8

Cuadrado A, Rojo AI, Wells G, Hayes JD, Cousin SP, Rumsey WL, Attucks OC, Franklin S, Levonen AL, Kensler TW, Dinkova-Kostova AT (2019) Therapeutic targeting of the NRF2 and KEAP1 partnership in chronic diseases. Nat Rev Drug Discov 18:295–317

Detienne G, Van de Walle P, De Haes W, Schoofs L, Temmerman L (2016) SKN-1-independent transcriptional activation of glutathione S-transferase 4 (GST-4) by EGF signaling. Worm 5:e1230585

Elmazoglu Z, Yar Saglam AS, Sonmez C, Karasu C (2020) Luteolin protects microglia against rotenone-induced toxicity in a hormetic manner through targeting oxidative stress response, genes associated with Parkinson's disease and inflammatory pathways. Drug Chem Toxicol 43:96–103

Eskandari MR, Mashayekhi V, Aslani M, Hosseini MJ (2015) Toxicity of thallium on isolated rat liver mitochondria: the role of oxidative stress and MPT pore opening. Environ Toxicol 30:232–241

Favari L, Mourelle M (1985) Thallium replaces potassium in activation of the (Na^+,K^+)-ATPase of rat liver plasma membranes. J Appl Toxicol 5:32–34

Flora SJ (2009) Structural, chemical and biological aspects of antioxidants for strategies against metal and metalloid exposure. Oxidative Med Cell Longev 2:191–206

Galván-Arzate S, Santamaría A (1998) Thallium toxicity. Toxicol Lett 99:1–13

Galván-Arzate S, Pedraza-Chaverrí J, Medina-Campos ON, Maldonado PD, Vázquez-Román B, Ríos C, Santamaría A (2005) Delayed effects of thallium in the rat brain: regional changes in lipid peroxidation and behavioral markers, but moderate alterations in antioxidants, after a single administration. Food Chem Toxicol 43:1037–1045

García E, Santana-Martínez R, Silva-Islas CA, Colín-González AL, Galván-Arzate S, Heras Y, Maldonado PD, Sotelo J, Santamaría A (2014) S-Allyl cysteine protects against MPTP-induced striatal and nigral oxidative neurotoxicity in mice: participation of Nrf2. Free Radic Res 48:159–167

Hanzel CE, Verstraeten SV (2006) Thallium induces hydrogen peroxide generation by impairing mitochondrial function. Toxicol Appl Pharmacol 216:485–492

Hanzel CE, Verstraeten SV (2009) Tl (I) and Tl (III) activate both mitochondrial and extrinsic pathways of apoptosis in rat pheochromocytoma (PC12) cells. Toxicol Appl Pharmacol 236:59–70

Harrington AJ, Hamamichi S, Caldwell GA, Caldwell KA (2010) *C. elegans* as a model organism to investigate molecular pathways involved with Parkinson's disease. Dev Dyn 239:1282–1295

Hassler CS, Chafin RD, Klinger MB, Twiss MR (2007) Application of the biotic ligand model to explain potassium interaction with thallium uptake and toxicity to plankton. Environ Toxicol Chem 26:1139–1145

Hauser-Davis RA, Comarú MW, Lopes RM (2020) Metallothionein determination can be applied to learn about aquatic metal pollution and oxidative stress detoxification mechanisms through problem-based learning. Biochem Mol Biol Educ doi. https://doi.org/10.1002/bmb.21342

Ke T, Aschner M (2019) Bacteria affect *Caenorhabditis elegans* responses to MeHg toxicity. Neurotoxicology 75:129–135

Khan MJ, Mukhtiar M, Qureshi MM, Jan SU, Ullah I, Hussain A, Khan MF, Gul R, Shahwani NA, Rabbani I (2018) Spectrophotometric investigation of glutathione modulation by thallium chloride in aqueous medium. Pakistan J Pharm Sci 31:1463–1467

Kim B, Emmons SW (2017) Multiple conserved cell adhesion protein interactions mediate neural wiring of a sensory circuit in *C. elegans*. Elife 6:e29257

Kim J-M, Chang HJ, Kim W-K, Chang N, Chun HS (2006) Structure-activity relationship of neuroprotective and reactive oxygen species scavenging activities for allium organosulfur compounds. J Agric Food Chem 54:6547–6553

Korotkov SM (2009) Effects of Tl^+ on ion permeability, membrane potential and respiration of isolated rat liver mitochondria. J Bioenerg Biomembr 41:277–287

Korotkov SM, Emelyanova LV, Konovalova SA, Brailovskaya IV (2015) Tl^+ induces the permeability transition pore in Ca^{2+}-loaded rat liver mitochondria energized by glutamate and malate. Toxicol in Vitro 29:1034–1041

Korotkov SM, Konovalova SA, Brailovskaya IV, Saris NE (2016) To involvement the conformation of the adenine nucleotide translocase in opening the Tl^+-induced permeability transition pore in Ca2+-loaded rat liver mitochondria. Toxicol in Vitro 32:320–332

Kotlar I, Colonnello A, Aguilera-González MF, Avila DS, de Lima ME, García-Contreras R, Ortíz-Plata A, Soares FAA, Aschner M, Santamaría A (2018) Comparison of the toxic effects of quinolinic acid and 3-nitropropionic acid in *C. elegans*: involvement of the SKN-1 pathway. Neurotox Res 33:259–267

Lin G, Sun Y, Long J, Sui X, Yang J, Wang Q, Wang S, He H, Luo Y, Qiu Z, Wang Y (2020) Involvement of the Nrf2-Keap1 signaling pathway in protection against thallium-induced oxidative stress and mitochondrial dysfunction in primary hippocampal neurons. Toxicol Lett 319:66–73

López-Diazguerrero NE, González Puertos VY, Hernández-Bautista RJ, Alarcón-Aguilar A, Luna-López A, Königsberg Fainstein M (2013) Hormesis: what doesn't kill you makes you stronger. Gac Med Mex 149:438–447

Lu C, Svoboda KR, Lenz KA, Pattison C, Ma H (2018) Toxicity interactions between manganese (Mn) and lead (Pb) or cadmium (Cd) in a model organism the nematode *C. elegans*. Environ Sci Pollut Res Int 25:15378–15389

Martinez-Finley EJ, Caito S, Slaughter JC, Aschner M (2013) The role of *skn-1* in methylmercury-induced latent dopaminergic neurodegeneration. Neurochem Res 38:2650–2660

Mattson MP (2008) Hormesis defined. Ageing Res Rev 7:1–7

Maya-López M, Mireles-García MV, Ramírez-Toledo M, Colín-González AL, Galván-Arzate S, Túnez I, Santamaría A (2018) Thallium-induced toxicity in rat brain crude synaptosomal/mitochondrial fractions is sensitive to anti-excitatory and antioxidant agents. Neurotox Res 33:634–640

McVey M (2010) Strategies for DNA interstrand crosslink repair: insights from worms, flies, frogs, and slime molds. Environ Mol Mutagen 51:646–658

Melnick RL, Monti LG, Motzkin SM (1976) Uncoupling of mitochondrial oxidative phosphorylation by thallium. Biochem Biophys Res Commun 69:68–73

Mulkey JP, Oehme FW (1993) A review of thallium toxicity. Vet Hum Toxicol 35:445–453

Nagashima T, Oami E, Kutsuna N, Ishiura S, Suo S (2016) Dopamine regulates body size in *Caenorhabditis elegans*. Dev Biol 412:128–138

Ogawa T, Kodera Y, Hirata D, Blackwell TK, Mizunuma M (2016) Natural thioallyl compounds increase oxidative stress resistance and lifespan in Caenorhabditis elegans by modulating SKN-1/Nrf. Sci Rep 6:21611

Osorio-Rico L, Villeda-Hernández J, Santamaría A, Königsberg M, Galván-Arzate S (2015) The N-methyl-D-aspartate receptor antagonist MK-801 prevents thallium-induced behavioral and biochemical alterations in the rat brain. Int J Toxicol 34:505–513

Osorio-Rico L, Santamaria A, Galván-Arzate S (2017) Thallium toxicity: general issues, neurological symptoms, and neurotoxic mechanisms. Adv Neurobiol 18:345–353

Pedraza-Chaverrí J, Gil-Ortiz M, Albarrán G, Barbachano-Esparza L, Menjívar M, Medina-Campos ON (2004) Garlic's ability to prevent in vitro Cu^{2+}-induced lipoprotein oxidation in human serum is preserved in heated garlic: effect unrelated to Cu^{2+}-chelation. Nutr J 3:10

Pino MTL, Marotte C, Verstraeten SV (2017) Epidermal growth factor prevents thallium(I)- and thallium(III)-mediated rat pheochromocytoma (PC12) cell apoptosis. Arch Toxicol 91:1157–1174

Pourahmad J, Eskandari MR, Daraei B (2010) A comparison of hepatocyte cytotoxic mechanisms for thallium (I) and thallium (III). Environ Toxicol 25:456–467

Queirós L, Pereira JL, Gonçalves FJM, Pacheco M, Aschner M, Pereira P (2019) *Caenorhabditis elegans* as a tool for environmental risk assessment: emerging and promising applications for a "nobelized worm". Crit Rev Toxicol 49:411–429

Rickwood CJ, King M, Huntsman-Mapila P (2015) Assessing the fate and toxicity of thallium I and thallium III to three aquatic organisms. Ecotoxicol Environ Saf 115:300–308

Ríos C, Galván-Arzate S, Tapia R (1989) Brain regional thallium distribution in rats acutely intoxicated with Tl_2SO_4. Arch Toxicol 63:34–37

Schetinger MRC, Peres TV, Arantes LP, Carvalho F, Dressler V, Heidrich G, Bowman AB, Aschner M (2019) Combined exposure to methylmercury and manganese during L1 larval stage causes motor dysfunction, cholinergic and monoaminergic up-regulation and oxidative stress in L4 *Caenorhabditis elegans*. Toxicology 411:154–162

Shashikumar S, Pradeep H, Chinnu S, Rajini PS, Rajanikant GK (2015) Alpha-linolenic acid suppresses dopaminergic neurodegeneration induced by 6-OHDA in *C. elegans*. Physiol Behav 151:563–569

Shi H, Jing X, Wei X, Perez RG, Ren M, Zhang X, Lou H (2015) S-allyl cysteine activates the Nrf2-dependent antioxidant response and protects neurons against ischemic injury *in vitro* and *in vivo*. J Neurochem 133:298–308

Soares MV, Puntel RL, Ávila DS (2018) Resveratrol attenuates iron-induced toxicity in a chronic post-treatment paradigm in *Caenorhabditis elegans*. Free Radic Res 52:939–951

Tang B, Tong P, Xue KS, Williams PL, Wang JS, Tang L (2019) High-throughput assessment of toxic effects of metal mixtures of cadmium(Cd), lead(Pb), and manganese(Mn) in nematode *Caenorhabditis elegans*. Chemosphere 234:232–241

Tao Z, Gameiro A, Grewer C (2008) Thallium ions can replace both sodium and potassium ions in the glutamate transporter excitatory amino acid carrier 1. Biochemistry 47:12923–12930

Tatsi K, Turner A, Handy RD, Shaw BJ (2015) The acute toxicity of thallium to freshwater organisms: implications for risk assessment. Sci Total Environ 536:382–390

Turner A, Furniss O (2012) An evaluation of the toxicity and bioaccumulation of thallium in the coastal marine environment using the macroalga, *Ulva lactuca*. Mar Pollut Bull 64:2720–2724

Twining BS, Twiss MR, Fisher NS (2003) Oxidation of thallium by freshwater plankton communities. Environ Sci Technol 37:2720–2726

Ushiama S, Ishimaru Y, Narukawa M, Yoshioka M, Kozuka C, Watanabe N, Tsunoda M, Osakabe N, Asakura T, Masuzaki H, Abe K (2016) Catecholamines facilitate fuel expenditure and protect against obesity via a novel network of the gut-brain axis in transcription factor skn-1-deficient mice. EBioMedicine 8:60–71

Verstraeten SV (2006) Relationship between thallium (I)-mediated plasma membrane fluidification and cell oxidants production in Jurkat T cells. Toxicology 222:95–102

Villaverde MS, Hanzel CE, Verstraeten SV (2004) In vitro interactions of thallium with components of glutathione-dependent antioxidant defence system. Free Radic Res 38:977–984